Zero-Bias Anomaly in a Nanowire Quantum Dot Coupled to Superconductors

Eduardo J. H. Lee,[1] Xiaocheng Jiang,[2] Ramón Aguado,[3] Georgios Katsaros,[1,*]
Charles M. Lieber,[2] and Silvano De Franceschi[1,†]

[1]SPSMS, CEA-INAC/UJF-Grenoble 1, 17 rue des Martyrs, 38054 Grenoble Cedex 9, France
[2]Harvard University, Department of Chemistry and Chemical Biology, Cambridge, Massachusetts 02138, USA
[3]Instituto de Ciencia de Materiales de Madrid, ICMM-CSIC Cantoblanco, 28049 Madrid, Spain
(Received 5 July 2012; published 31 October 2012)

We studied the low-energy states of spin-1/2 quantum dots defined in InAs/InP nanowires and coupled to aluminum superconducting leads. By varying the superconducting gap Δ with a magnetic field B we investigated the transition from strong coupling $\Delta \ll T_K$ to weak-coupling $\Delta \gg T_K$, where T_K is the Kondo temperature. Below the critical field, we observe a persisting zero-bias Kondo resonance that vanishes only for low B or higher temperatures, leaving the room to more robust subgap structures at bias voltages between Δ and 2Δ. For strong and approximately symmetric tunnel couplings, a Josephson supercurrent is observed in addition to the Kondo peak. We ascribe the coexistence of a Kondo resonance and a superconducting gap to a significant density of intragap quasiparticle states, and the finite-bias subgap structures to tunneling through Shiba states. Our results, supported by numerical calculations, own relevance also in relation to tunnel-spectroscopy experiments aiming at the observation of Majorana fermions in hybrid nanostructures.

DOI: 10.1103/PhysRevLett.109.186802 PACS numbers: 73.21.La, 72.15.Qm, 73.63.Kv, 74.45.+c

Hybrid devices which couple superconducting (S) electrical leads to low-dimensional semiconductors have received great attention due to their fascinating underlying physics [1]. Further interest in this field has been generated by recent theoretical predictions on the existence of Majorana fermions at the edges of one-dimensional semiconductor nanowires (NWs) with strong spin-orbit interaction connected to S electrodes [2]. Zero-bias conductance peaks meeting some of the expected characteristic signatures of Majorana physics were recently reported in hybrid devices based on InSb [3,4] and InAs NWs [5]. In the past years, quantum dots (QDs) coupled to superconducting leads have been widely explored as tunable Josephson junctions [6,7], or as building blocks of Cooper-pair splitters [8–10]. Hybrid superconductor-QD devices also constitute versatile platforms for studying fundamental issues, such as the physics of the Andreev bound states (ABS) [11–13] or the interplay between the Kondo effect and the superconducting proximity effect [14–16,16–24].

The Kondo effect usually stems from the antiferromagnetic coupling of a localized electron spin and a Fermi sea of conduction electrons. Below a characteristic temperature T_K, the so-called Kondo temperature, a many-body spin-singlet state is formed, leading to the partial or complete screening of the local magnetic moment. This phenomenon, discovered in metals containing diluted magnetic impurities, is now routinely found in individual QDs with a spin-degenerate ground state, e.g., QDs hosting an odd number of electrons. The Kondo effect manifests itself as a zero-bias conductance peak whose width is proportional to T_K. In S-QD-S devices, the quasiparticle density of states (DOS) around the Fermi level (E_F) of the leads vanishes due to the opening of the superconducting gap (Δ). This lack of quasiparticles precludes Kondo screening.

The competition between the Kondo effect and superconductivity is governed by the corresponding energy scales, $k_B T_K$ and Δ. While no Kondo screening occurs for $k_B T_K \ll \Delta$ (weak coupling), a Kondo singlet is expected to form for $k_B T_K \gg \Delta$ (strong coupling) at the expense of the breaking of Cooper pairs at the Fermi level [18,25]. A quantum phase transition is predicted to take place at $k_B T_K \approx \Delta$ [15–17]. Experimental signatures of this exotic crossover have been investigated both in the Josephson supercurrent regime [21–23] and in the dissipative subgap transport regime [18–20]. Yet a full understanding of these experimental findings is still lacking. In this Letter, we report an experimental study on S-QD-S devices where the relative strength between Kondo and superconducting pairing correlations is tuned by means of a magnetic field B acting on Δ. The transition from strong to weak coupling is continuously achieved by sweeping B from above the critical field B_c, where $\Delta = 0$, to zero field, where Δ attains its maximum value Δ_0 exceeding $k_B T_K$.

The S-QD-S devices were fabricated from individual InAs/InP core/shell NWs grown by thermal evaporation (total diameter $\approx$30 nm). The InP shell (thickness $\approx$ 2 nm) acts as a confinement barrier resulting in an enhanced mobility of the one-dimensional electron gas in the InAs core [26]. After growth, the NWs were deposited onto a degenerately doped, p-type Si substrate (used as a back gate), covered by a 300-nm-thick thermal oxide. Device fabrication was accomplished by e-beam lithography, Ar^+ bombardment (to remove native oxides), metal evaporation, and lift-off. Source and drain contacts consisted of Ti (2.5 nm)/Al (45 nm) bilayers with a lateral separation of approximately 200 nm, and a superconducting critical temperature of ≈1 K. Transport measurements were performed in a He_3-He_4 dilution refrigerator with a base temperature of 15 mK.

At low temperature, electron transport is dominated by Coulomb blockade with the NW channel behaving as a single QD. Charge stability measurements (i.e., differential conductance dI/dV as a function of source-drain bias V_{sd} and back-gate voltage V_G) were performed to identify Kondo resonances in Coulomb diamonds with a spin-1/2 ground state. These measurements were taken at 15 mK with the leads in the normal state (superconductivity was suppressed by means of a magnetic field $B^\perp = 70$ mT perpendicular to the substrate and exceeding the perpendicular critical field $B_c^\perp$). In each Kondo diamond, T_K was measured from the half width at half maximum of the zero-bias dI/dV peak, while the tunnel coupling asymmetry was extracted from the peak height, i.e., the linear conductance G, according to the relation: $G/G_0 = 4\Gamma_L\Gamma_R/(\Gamma_L + \Gamma_L)^2$, where $G_0 = 2e^2/h$ and $\Gamma_{L(R)}$ is the tunnel coupling to the left (right) lead. Here we present data corresponding to three Kondo diamonds labeled as α, β, and γ, where $T_{K,\alpha} \approx 0.56$ K, $(\Gamma_L/\Gamma_R)_\alpha \approx 6.6 \times 10^{-3}$, $T_{K,\beta} \approx 1$ K, $(\Gamma_L/\Gamma_R)_\beta \approx 0.44$, and $T_{K,\gamma} \approx 0.71$ K, $(\Gamma_L/\Gamma_R)_\gamma \approx 7.6 \times 10^{-3}$.

Figure 1(a) shows a $dI/dV(B^\perp, V_{sd})$ measurement taken at the center of Kondo diamond α. The zero-bias Kondo peak is apparent above $B_c^\perp \approx 23$ mT (we note that at such low fields the Zeeman splitting is much smaller than $k_B T_{K,\alpha}$, explaining the absence of a split Kondo peak). Surprisingly, reducing the field below $B_c^\perp$ does not lead to an abrupt suppression of the Kondo peak. Instead, the peak becomes progressively narrower and smaller, vanishing completely only below $B^\perp \approx 9$ mT.

We argue that the observed zero-bias peak is a manifestation of Kondo screening due to intragap quasiparticle states. To support this interpretation, we show in Fig. 1(b) a data set taken in an adjacent diamond with even occupation (i.e., with no Kondo effect). The $dI/dV(V_{sd})$ traces shown correspond to different in-plane fields, $B^\parallel$, ranging from zero to just above the in-plane critical field $B_c^\parallel \approx 200$ mT. When lowering the fields from above to below $B_c^\parallel$, the subgap dI/dV does not drop abruptly, supporting our hypothesis of a sizable quasiparticle DOS at E_F [we note that, although the measurement of Fig. 1(b) refers to in-plane fields, a qualitatively similar behavior can be expected for perpendicular fields, see Supplemental Material [27]]. The development of a "soft" gap just below $B_c^\parallel$ is additionally marked by the absence of dI/dV peaks characteristic of the BCS DOS singularities (a discussion of the origin of the soft gap is included in the Supplemental Material [27]). Such peaks develop only

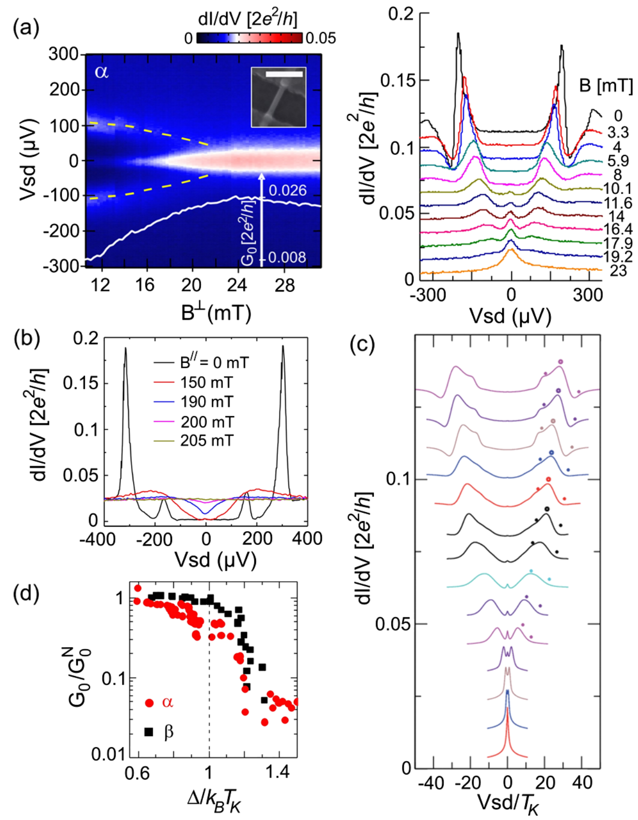

FIG. 1 (color online). (a) Left panel: Color plot of dI/dV vs $(B^\perp, V_{SD})$ measured at the center of diamond α. The dashed lines highlight the emergence of finite-bias peaks related to the opening of a superconducting gap. The superimposed line trace shows the $B^\perp$ dependence of the linear conductance. Right panel: $dI/dV(V_{SD})$ traces taken at different $B^\perp$ values. The inset shows a scanning electron micrograph of a typical device (scale bar: 200 nm). (b) $dI/dV(V_{SD})$ traces measured in an even diamond revealing the Dynes-like DOS of leads. (c) Numerical calculations. The smaller solid dots denote the position of the Δ and 2Δ peaks, whereas the open dots highlight the position of the Shiba bound state peaks. (d) Linear conductance (G_0) normalized to the normal-state value (G_0^N) and plotted as a function of $\Delta/k_B T_K$ for diamonds α (red dots) and β (black squares).

at fields well below $B_c^\parallel$, becoming most pronounced at $B = 0$. In this low-field limit, the subgap conductance simultaneously vanishes and first-order multiple-Andreev-reflection resonances emerge at $eV_{sd} \approx \pm\Delta$.

To reproduce the observed subgap features and the coexistence of a Kondo peak and a superconducting gap, we calculated the dI/dV of a QD modeled by an Anderson Hamiltonian including coupling to BCS-type superconducting reservoirs. We used the so-called noncrossing approximation, a fully nonperturbative theory that includes both thermal and quantum fluctuations, complemented with the Keldysh-Green's function method to take into account nonequilibrium effects at finite V_{sd} (see Supplemental Material [27]). In order to fit the experimental data, the DOS of the leads was modeled by a Dynes function:

$$N_s(E, \gamma, B) = \mathrm{Re}\left[\frac{|E| + i\gamma(B)}{\sqrt{(|E| + i\gamma(B))^2 - \Delta(B)^2}}\right], \quad (1)$$

where $\gamma(B)$ is a phenomenological broadening term [28]. For small $\Delta(B)$, the $\gamma(B)$ term is particularly important leading to a finite quasiparticle DOS at E_F. By contrast, as $\Delta(B)$ increases (with decreasing B), the DOS of the superconducting leads approaches the ideal BCS profile.

Figure 1(c) shows a set of calculated $dI/dV(V_{\rm sd})$ traces at different B. By adjusting the DOS parameters $\gamma(B)$ and $\Delta(B)$, these calculations clearly show a zero-bias peak persisting below the B_c, in agreement with the experimental data of Fig. 1(a). Since this peak emerges only in the case of a finite $\gamma(B)$, we conclude that the finite DOS at the Fermi level is at the origin of the experimentally observed zero-bias anomaly. The narrowing of this Kondo anomaly with increasing Δ can be interpreted as a decreasing T_K due to the shrinking quasiparticle DOS around the Fermi level (this aspect is more quantitatively discussed in the Supplemental Material [27]). As T_K approaches the electronic temperature, the peak height gets smaller leading to the disappearance of the zero-bias peak.

Figure 2 shows a second data set taken in Kondo diamond β. In this case, the stronger and more symmetric coupling to the leads results in a higher T_K, and a larger peak conductance. Nevertheless, the field dependence [Fig. 2(a)] shows substantially the same behavior as in Fig. 1(a), i.e., a zero-bias Kondo peak persisting below $B_c^\perp$, becoming progressively narrower with decreasing $B^\perp$, and vanishing below $B^\perp \approx 10$ mT. Interestingly, a sharp dI/dV resonance is found around $V_{\rm sd} = 0$ superimposed to the (wider) zero-bias Kondo peak. This resonance persists throughout the entire field range in which the leads are superconducting. By performing current-bias measurements [inset of Fig. 2(b)], we were able to ascribe this sharp resonance to a Josephson supercurrent as high as 0.9 nA at $B = 0$. This finding reveals the possibility of a coexistence between the Josephson effect, linked to the superconducting nature of the leads, and a Kondo effect

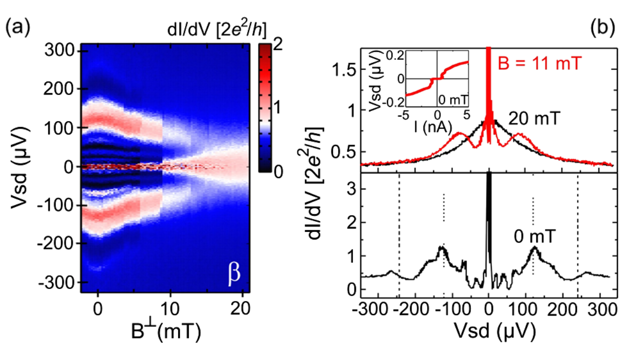

FIG. 2 (color online). (a) $B^\perp$ dependence measured in diamond β. (b) dI/dV line profiles taken at different B. The inset is a voltage-current measurement carried out at $B = 0$, which reveals transport of a dissipationless supercurrent in the device.

arising from the exchange coupling between the localized electron and intragap quasiparticle states.

The peak heights of Kondo resonances α and β appear to follow approximately the same dependence on $\Delta/k_B T_K$ [Fig. 1(d)], where T_K refers to the Kondo temperature in the normal state. A similar scaling was reported earlier by Buizert *et al.* [18], for a S-QD-S device fabricated from an InAs self-assembled QD using Ti/Al contacts. In that Letter, it was speculated that when $k_B T_K \gg \Delta$, it becomes energetically favorable for Cooper pairs to split in order to screen the local spin and create a Kondo resonance at the Fermi level. The results presented here point at a different interpretation based on the presence of the already discussed intragap quasiparticle states, which become particularly important when B approaches B_c. According to this interpretation, the apparent scaling in Fig. 1(d) is intimately related to a quasiparticle "poisoning" of the superconducting gap.

Well below B_c, as the Kondo anomaly disappears, the $dI/dV(V_{\rm sd})$ is dominated by a pair of peaks symmetrically positioned with respect to $V_{\rm sd} = 0$ [Fig. 1(a)]. These peaks become most pronounced at $B = 0$. Similar types of subgap structures (SGS) have been reported in earlier works and were given different interpretations: a Kondo enhancement of the first order Andreev reflection process [18–20], or, in the case of asymmetrically coupled S-QD-S devices, a persisting Kondo resonance, created by the strongly coupled lead, which is probed by the BCS DOS of the second, weakly coupled lead [19]. Some of the above interpretations [18,19] invoke Kondo correlations to explain the observed subgap structure, even though, as we have pointed out, these correlations get suppressed as Δ reaches its largest value at $B = 0$.

More recently, finite-bias SGS were explained in terms of tunneling through Yu-Shiba-Rusinov states [29,30]. These intragap bound states, often referred to as Shiba states, were originally discussed in the case of magnetic impurities embedded in a superconductor [31–34]. They can be seen as ABS emerging as a result of the exchange coupling J between the impurity and the superconductor. As later confirmed by experiments based on scanning tunneling spectroscopy [35], Shiba states emerge as pairs of peaks in the local DOS symmetrically positioned at energies $\pm E_B$ relative to the Fermi level, where E_B depends on J and $|E_B| < \Delta$.

The zero-field $dI/dV(V_{\rm sd})$ trace in the right panel of Fig. 1(a) exhibits a pair of dI/dV peaks at $eV_{\rm sd} \approx \pm 1.4\Delta$, followed by negative dI/dV regions. Taking into account the strong asymmetry in the tunnel couplings, these features can be well explained in terms of a pair of Shiba levels with $E_B = 0.4\Delta$, created by the strongly coupled S lead, and tunnel probed by the weakly coupled S lead [see Fig. 3(a)]. The observed dI/dV peaks result from the alignment of these Shiba levels with the BCS gap-edge singularities. Precisely, one dI/dV peak is due to the onset

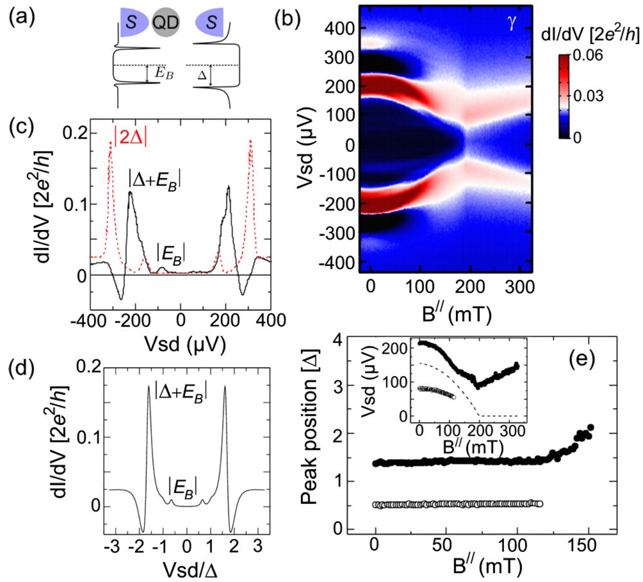

FIG. 3 (color online). (a) Schematics of the formation of Yu-Shiba-Rusinov bound states resulting from the interaction of the QD with the strongly coupled lead. (b) $B^{\parallel}$ dependence of dI/dV measured in diamond γ. (c) The solid line depicts the dI/dV taken at $B = 0$. Two pairs of peaks are observed at $|eV_{\mathrm{sd}}| = \Delta + E_B, E_B$. The dashed line shows the equivalent dI/dV taken in an even diamond, for comparison. (d) Numerical calculation of the dI/dV for $B = 0$. (e) Position of the intragap peaks as a function of B. The inset shows the data before performing the rescaling in units of Δ. The dashed line displays the field dependence of Δ.

of electron tunneling from the Shiba level below E_F to the empty quasiparticle band of the S probe. The other peak is due to the onset of electron tunneling from the occupied quasiparticle band of the S probe to the Shiba level above E_F. Increasing $|V_{\mathrm{sd}}|$ beyond these resonance conditions leads to a reduced tunneling probability and hence a negative dI/dV. The Shiba-related features observed in Fig. 1(a) are very well reproduced by the numerical results in Fig. 1(c). In the case of relatively low contact asymmetry [lower panel of Fig. 2(b)], both S leads interact with the QD spin resulting in a stronger J. We find a pair of dI/dV peaks at $eV_{\mathrm{sd}} \approx \pm\Delta$, which implies $E_B \approx 0$. In addition, we observe a rather complex set of smaller peaks most likely due to multiple-Andreev-reflection processes.

In the weak-coupling limit, the energy of the Shiba states is related to Δ through $E_B = \Delta(1 - x)/(1 + x)$, where $x = 3(\pi\nu_F J/4)^2$ and ν_F is the Fermi velocity [30]. Since J is presumably independent of B, the energy of the Shiba states should evolve proportionally to $\Delta(B)$ as B is varied. We have verified this dependence with a measurement performed in diamond γ, where, as in diamond α, tunnel couplings are strongly asymmetric. Differently from diamond α, however, the low-energy transport is characterized by two pairs of intragap dI/dV peaks, as shown by the zero-field curve in Fig. 3(c). As in Fig. 1(a), the most prominent peaks (at $eV_{\mathrm{sd}} \sim \pm1.4\Delta$) correspond to the alignment of the Shiba levels with the BCS coherence peaks of the weakly coupled contact, and they are consistently followed by negative dI/dV dips. The weaker peaks at $eV_{\mathrm{sd}} \approx \pm0.53\Delta$ (in fact only one of them is clearly visible) can be interpreted as "replicas" of the Shiba peaks. Such replicas are expected when the Shiba levels line up with the Fermi level of the weakly coupled S lead (for $eV_{\mathrm{sd}} = \pm E_B$), provided a non negligible density of quasiparticles is present throughout its superconducting gap. This is apparent from the calculated $dI/dV(V_{\mathrm{sd}})$ trace in Fig. 3(d), which agrees fairly well with the experimental one.

The Shiba peaks and their replicas shift towards $V_{\mathrm{sd}} = 0$ as $B^{\parallel}$ is increased. Their positions are plotted in the inset of Fig. 3(e) as solid and open dots, respectively. For comparison, the $\Delta(B^{\parallel})$ dependence measured in a non-Kondo diamond is also plotted. Up to $B^{\parallel} \sim 120$ mT, the Shiba peaks and their replicas evolve proportionally to $\Delta(B^{\parallel})$ in agreement with the theoretical prediction. Above $B^{\parallel} \sim 120$ mT, this behavior begins to be affected by the increasing Zeeman splitting (≈ 0.3 meV/T) of the QD spin doublet. The main Shiba peaks get strongly suppressed and they seem to eventually merge into the normal-state, Zeeman-split Kondo peaks through a nontrivial transition region (roughly between 120 and 180 mT). This large Zeeman splitting prevents the observation of a zero-bias Kondo peak when approaching $B_c^{\parallel}$.

In conclusion, we have studied the transport properties of a spin-1/2 QD coupled to S contacts. The ability to continuously tune Δ with an external magnetic field enabled us to investigate the transition from a normal-state Kondo to a superconducting-state Shiba ground state. We showed that the presence of a finite quasiparticle DOS within Δ can promote the formation of a zero-bias Kondo peak coexisting with superconductivity. The origin of this quasiparticle DOS remains to be clarified, also through a better understanding of the superconducting proximity effect in semiconductor NW structures (e.g., the role of disorder-induced pair breaking [36]). Finally, we should like to emphasize that our results bear clear implications in the interpretation of subgap transport features in hybrid superconductor-semiconductor systems, especially in the presence of relatively high B that can cause a significant suppression of Δ. This is precisely the regime where Majorana fermions are expected to arise as zero-energy quasiparticle states. We argue that intragap quasiparticle states, manifesting through a sizable background conductance (as seen in Refs. [3–5]), could result in the screening of a local spin (or orbital) degeneracy leading to zero-bias anomalies that are not related to Majorana physics.

This work was supported by the EU Marie Curie program and by the Agence Nationale de la Recherche. R. A. acknowledges support from the Spanish Ministry of Science and Innovation through Grant No. FIS2009-08744.

*Present address: Johannes Kepler University, Institute of Semiconductor and Solid State Physics, Altenbergstr. 69, A-4040 Linz, Austria.

†silvano.defranceschi@cea.fr

[1] S. D. Franceschi, L. P. Kouwenhoven, C.Schönenberger, and W. Wernsdorfer, Nature Nanotech. **5**, 703 (2010).

[2] R. M. Lutchyn, J. D. Sau, and S. Das Sarma, Phys. Rev. Lett. **105**, 077001 (2010).

[3] V. Mourik, K. Zuo, S. M. Frolov, S. R. Plissard, E. P. A. M. Bakkers, and L. P. Kouwenhoven, Science **336**, 1003 (2012).

[4] M. T. Deng, C. L. Yu, G. Y. Huang, M. Larsson, P. Caroff, and H. Q. Xu, arXiv:1204.4130v1.

[5] A. Das, Y. Ronen, Y. Most, Y. Oreg, M. Heiblum, and H. Shtrikman, arXiv:1205.7073v1.

[6] J. A. van Dam, Y. V. Nazarov, E. P. A. M Bakkers, S. D. Franceschi, and L. P. Kouwenhoven, Nature (London) **442**, 667 (2006).

[7] J. Cleuziou, W. Wernsdorfer, V. Bouchiat, T. Ondarcuhu, and M. Monthioux, Nature Nanotech. **1**, 53 (2006).

[8] L. Hofstetter, S. Csonka, J. Nygård, and C. Schönenberger, Nature (London) **461**, 960 (2009).

[9] L. G. Herrmann, F. Portier, P. Roche, A. L. Yeyati, T. Kontos, and C. Strunk, Phys. Rev. Lett. **104**, 026801 (2010).

[10] A. Das, Y. Ronen, M. Heiblum, D. Mahalu, A. V. Kretinin, and H. Shtrikman, arXiv:1205.2455v1.

[11] J.-D. Pillet, C. H. L. Quay, P. Morfin, C. Bena, A. Levy Yeyati, and P. Joyez, Nat. Phys. **6**, 965 (2010).

[12] R. S. Deacon, Y. Tanaka, A. Oiwa, R. Sakano, K. Yoshida, K. Shibata, K. Hirakawa, and S. Tarucha, Phys. Rev. Lett. **104**, 076805 (2010).

[13] T. Meng, S. Florens, and P. Simon, Phys. Rev. B **79**, 224521 (2009).

[14] M. R. Buitelaar, T. Nussbaumer, and C. Schönenberger, Phys. Rev. Lett. **89**, 256801 (2002).

[15] F. Siano and R. Egger, Phys. Rev. Lett. **93**, 047002 (2004).

[16] M. S. Choi, M. Lee, K. Kang, and W. Belzig, Phys. Rev. B **70**, 020502(R) (2004).

[17] A. Oguri, Y. Tanaka, and A. C. Hewson, J. Phys. Soc. Jpn. **73**, 2494 (2004).

[18] C. Buizert, A. Oiwa, K. Shibata, K. Hirakawa, and S. Tarucha, Phys. Rev. Lett. **99**, 136806 (2007).

[19] A. Eichler, M. Weiss, S. Oberholzer, C. Schönenberger, A. Levy Yeyati, J. C. Cuevas, and A. Martin-Rodero, Phys. Rev. Lett. **99**, 126602 (2007).

[20] T. Sand-Jespersen, J. Paaske, B. M. Andersen, K. Grove-Rasmussen, H. I. Jørgensen, M. Aagesen, C. B. Sørensen, P. E. Lindelof, K. Flensberg, and J. Nygård, Phys. Rev. Lett. **99**, 126603 (2007).

[21] Y. Kanai, R. S. Deacon, O. Oiwa, K. Yoshida, K. Shibata, K. Hirakawa, and S. Tarucha, Phys. Rev. B **82**, 054512 (2010).

[22] K. Grove-Rasmussen, H. Jørgensen, and P. Lindelof, New J. Phys. **9**, 124 (2007).

[23] A. Eichler, R. Deblock, M. Weiss, C. Karrasch, V. Meden, C. Schönenberger, and H. Bouchiat, Phys. Rev. B **79**, 161407 (2009).

[24] K. J. Franke, G. Schulze, and J. I. Pascual, Science **332**, 940 (2011).

[25] L. I. Glazman and K. Matveev, JETP Lett. **49**, 659 (1989).

[26] X. Jiang, Q. Xiong, F. Qian, Y. Li, and C. M. Lieber, Nano Lett. **7**, 3214 (2007).

[27] See Supplemental Material at http://link.aps.org/supplemental/10.1103/PhysRevLett.109.186802 for details of the theoretical model, a discussion of the origin of the soft gaps, and temperature dependence data of the zero-bias anomaly.

[28] In our modeling we used $\gamma(B) = 0.4(B/B_c)\Delta(B)$. This simple function captures the experimentally observed field-induced increase in the broadening of the BCS coherence peaks and in the quasiparticle DOS at the Fermi level [both linked to the $\gamma(B)/\Delta(B)$ ratio].

[29] V. Koerting, B. M. Andersen, K. Flensberg, and J. Paaske, Phys. Rev. B **82**, 245108 (2010).

[30] B. M. Andersen, K. Flensberg, V. Koerting, and J. Paaske, Phys. Rev. Lett. **107**, 256802 (2011).

[31] L. Yu, Acta Phys. Sin. **21**, 75 (1965).

[32] H. Shiba, Prog. Theor. Phys. **40**, 435 (1968).

[33] A. I. Rusinov, Zh. Eksp. Teor. Fiz. **56**, 2047 (1969) [Sov. Phys. JETP **29**, 1101 (1969)].

[34] A. V. Balatsky, I. Vekhter, and J. X. Zhu, Rev. Mod. Phys. **78**, 373 (2006).

[35] A. Yazdani, B. A. Jones, C. P. Lutz, M. F. Crommie, and D. M. Eigler, Science **275**, 1767 (1997).

[36] J. Liu, A. C. Potter, K. T. Law, and P. A. Lee, arXiv:1206.1276v1.